EMPRO

Current Research in Pharmaceutical Sciences

Available online at www.crpsonline.com

ISSN: 2250 – 2688

Received: 29/04/2020
Revised: 20/05/2020
Accepted: 25/05/2020
Published: 08/07/2020

Darshana Gohate
Department of Pharmacy, Barkatullah University, Bhopal (M.P), India 462026

Parul Mehta
School of Pharmacy, LNCT University, Kolar, Bhopal

Correspondence

Darshana Gohate
Department of Pharmacy, Barkatullah University, Bhopal (M.P), India 462026

Email: darshanaiswe@gmail.com

DOI: 10.24092/CRPS.2020.100202

Website: www.crpsonline.com

Quick Response Code:

2D and 3D QSAR Analysis of Imidazole Derivatives as Heme Oxygenase Inhibitor

Darshana Gohate and Parul Mehta

ABSTRACT

Selective inhibition of heme oxygenase is an important strategy in design of potent inhibitors of enzyme for the treatment of neonatal jaundice, cancer and many more. QSAR analysis is employed for a given set of compounds containing imidazole pharmacophore in order to establish a relationship between the biological activity and related descriptors, which provides us an idea to gain a potent inhibitor with lesser side effects. In this paper we present results of 2D and 3D QSAR studies of series of 26 molecules containing imidazole pharmacophore as selective heme oxygenase inhibitor using V Life MDS 3.5 Software. The 2D QSAR studies was performed using Partial Least Square Regression method and the 3D QSAR studies was performed using k- Nearest Neighbor Molecular Field Analysis(kNN- MFA) method. The analysis has produced good predictive and statistically significant QSAR models. 2D QSAR studies produced good statistical model with r^2 value 0.8487, cross validated r^2 value 0.6553 and prd_r^2 value 0.7478 by PLSR method while 3D QSAR model gave statistical value of cross validated r^2 value 0.5493 and pred_r^2 value 0.3358. The results of the QSAR analysis suggested that the 2-D descriptor viz. physicochemical and alignment independent played an important role for heme oxygenase inhibition and the 3-D descriptors electrostatic and steric revealed the relative positions and range for substitution in a molecule. In 3D model, grid suggested that a positive electrostatic potential is favorable for increase in biological activity and the steric field with negative range and the negative range indicates that negative steric potential is favorable for increase in the activity. Thus, the descriptors generated by 2-D and 3-D QSAR analysis were useful in designing of potent molecules.

Key words: Heme Oxygenase Inhibitor; HO-1; 2D QSAR; 3D QSAR; kNN-MFA

1. INTRODUCTION

Heme Oxygenase (HO) (EC 1.14.99.3) catalyses the first and rate-limiting step in the oxidative breakdown of heme to carbon monoxide (CO), biliverdin (which is rapidly reduced to bilirubin), and ferrous iron.[1,2,3] Heme Oxygenase Inhibitor is highligtened in case of neonatal jaundice, [4,5,6,7,8] intracerebral hemorrhage,[9,10,11] as an anticancer agent [12,13,14] and many more. Various Heme Oxygenase inhibitors are being made till date like metalloporphyrins[15,16,17] and imidazole-dioxolane compounds [18,19,20.21]. Our present focus is to make a potent inhibitor which is helpful to us in the neonatal jaundice which is a severe pathological condition exhibited in neonates, and can also lead to drastic condition of brain damage i.e.'kernicterus'. Also, our main emphasis is to examine potential applications of pharmacologic inhibitors of HO activity as therapeutic agents in the context of disease processes associated with excessive activation of heme oxygenase system. So, there is a need to design and screen heme oxygenase inhibitors with higher bioactivities. There is a need to analyze the correlation between heme oxygenase inhibitor activity and physico-chemical parameters of each category of compounds using the Quantitative Structure Activity Relationship (QSAR) methods because the quantitative analysis of such molecules can be utilized for increasing the potency and minimizing the side effects.

Imidazole is an organic compound with the formula $C_3H_4N_2$. This aromatic heterocyclic is classified as an alkaloid. Imidazole ring system is present in important biological building blocks such as histidine, and the related hormone histamine. It has a wide range of pharmacological activity like antifungal,[22] antimycobacterial,[23]antiprotozoal,[24] analgesic,[25] anticancer,[26] angiotensin antagonist,[27] antidepressant,[28] antihistaminic,[29] antihypertensive [30] and as heme oxygenase inhibitor.[31,32,33,34,35] Various researches are being going on imidazole-dioxolane compounds as heme oxygenase inhibitor, so QSAR analysis will help us to predict some newer potent molecule in order to study and establish a correlation between structure and biological activity of imidazole-dioxolane, as heme oxygenase inhibitors.

2. MATERIALS AND METHODS

2.1 Data Set

The Heme Oxygenase Inhibition of imidazole-dioxolane, figure 1 has been reported by Vlahakis *et al*., [36] in terms of inhibitory concentration 50% of enzyme Heme Oxygenase-1 [HO-1] (IC_{50} in micromoles). One of the compounds of the series has no well defined activity, so the QSAR study was performed on a set of 25 molecules. The enzyme inhibition data were converted to negative logarithmic pIC_{50} to reduce skewness of dataset and then used for subsequent QSAR analysis as dependent variables. The structures of all imidazole analogues with HO-1 inhibitory activity are presented in Table no-1. All computational studies were performed using V–Life Molecular Design Software Version 3.5.[37] The sketched structures were then exported to three dimensional structures (3D). The geometries of generated 3D structures were optimized using Merck Molecular Force Field (MMFF) fixing Root Mean Square Gradients (RMS) to 0.01 Kcal/mol Å as implemented in the V-Life MDS 3.5.

2.2 2D QSAR

The QSAR models were generated by using biological activity as dependent variable and descriptors as independent variables. The series of compounds were divided into test and training set for the generation of models. In present study, manual selection method is applied, using Partial Least Square [PLS], with forward- backward variable selection method. The program employs a stepwise technique, i.e., only one parameter at a time was added to a model and always in the order of most significant to least significant in terms of F-test values. Statistical parameters were calculated subsequently for each step in the process, so the significance of the added parameter could be verified. The goodness of the correlation is tested by the regression coefficient (r^2), the cross-validated squared correlation co-efficient (q^2), the F-test and the standard error of estimate (SEE). The correlation coefficient values closer to 1.0 represent the better fit of the model. The F-test reflects the ratio of the variance explained by the model and the variance due to the error in the model (i.e.,the variance not explained by the model). High values of the F-test indicate that the model is statistically significant. The predictive r^2 (r^2pred) was calculated for evaluating the predictive capacity of the model. The value of pred$r^2 \geq 0.5$ indicates the good predictive capacity of the QSAR model. It has been observed that the values of statistical parameters like $q^2 \geq 0.5$ and prd$r^2 \geq 0.5$ was not achieved in models generated, also from the fitness plot of the generated model, 2 molecules were considered outliers, so it has been removed from the data set and further the models were regenerated. After removal of outliers, a good statistical result was observed.

2.3 3D QSAR

Molecular alignment utility allows alignment of two or more molecules in a dataset with respect to selected template or with respect to a particular set of atoms explicitly selected in every molecule of the data set. The resulting set of aligned molecules can then be used in the 3D-QSAR for building quantitative models to predict new molecules having the similar template or set of atoms. Molecular alignment is also used in visualizing the structural diversity in the given set of molecules. Template Based alignment method was used for the generation of model. Template Based Alignment feature performs alignment of set of molecules based on given template. A reference molecule is selected for defining coordinates to align rest of the molecules. The aligned molecules are automatically stored in the reference folder. Set of molecules lacking common template can also be aligned based on a set of atoms selected in same order in all the molecules of the set. In the present study imidazole template was considered (figure 2) and the alignment was observed (figure 3).

Aligned molecules were used to calculate 3-D descriptor with biological activity as dependent variable. Before calculation of 3-D descriptors following values and parameters are to be fixed like field type as electrostatic, steric and hydrophobic. Charge type set as Gasteiger- Marsili, dielectric constant as 1.0 with distance dependent dielectric function. A sp3 carbon atom and + 1.0 charge was served as the probe atom to calculate steric and electrostatic fields. The grid setting is given below (Table 2).

The QSAR models were generated using k-nearest neighbor method (kNN) of V Life molecular design suite.[38] The test set of 7 molecules and a training set of 16 molecules were subjected to 3D QSAR analysis. The kNN-MFA model provided direction for the design of new molecules in a rather convenient way. The kNN-MFA model show the grid which shows the point contributes stepwise kNN-MFA. The range of property values for the chosen points may aid in the design of new potent molecules.

The range is based on the variation of the field values at the chosen points using the most active molecule and its nearest neighbor set.

3. RESULTS & DISCUSSION

3.1 2D–QSAR studies

QSAR analysis on a series of imidazole-dioxolane was performed by using V-Life software. The physiochemical descriptors and inhibitory activity was taken as independent and dependent variables respectively. Correlations were established between the biological activity and calculated molecular physiochemical descriptors through Partial Least Square regression (Stepwise forward-backward). The summary of model is given below:

Equation: PIC50 = -1.2583 T_N_O_7 -0.0075 Mol.Wt. + 0.1232 SsNH2E-index + 0.5912 T_O_F_5 + 3.0766

Statistics: n= 18; r^2 = 0.8487, q^2 = 0.6553, prd r^2 = 0.7478, r^2se = 0.2055, q^2se = 0.3102, prd r^2 se = 0.1988, F test = 42.0756.

The statistics of the generated model explains 84.87% (r^2 = 0.8487) of the total variance in the training set as well as it has internal (q^2) and external (prd_r^2) predictive ability of 65% and 74% respectively. The low standard error r^2se = 0.2055, q^2se = 0.3102 and prdr^2se= 0.1988 demonstrates accuracy of the model. The F test = 42.0756 shows the statistical significance of 99.99% of the model which means that probability of failure of the model is 1 in 10000.

The descriptors: mol. wt. signifies molecular weight of compounds, SsNH2E-index signifies Electro topological state indices for number of $–NH_2$ group connected with one single bond, T_N_O_7 signifies the count of number of nitrogen atom separated from oxygen atom by 7 bonds in a molecule, T_O_F_5 signifies the count of number of oxygen atom separated from fluorine atom by 5 bonds in a molecule. The developed PLSR model reveals that the descriptors T_N_O_7, Mol. Wt., SsNH2E-index and T_O_F_5 were highly correlated to biological activity (Figure 4).The descriptor T_N_O_7 (i.e. the count of number of nitrogen atom separated from oxygen atom by 7 bonds in a molecule) plays most important role (-39.28%) and is inversely proportional to the biological activity. A negatively correlated descriptor Mol. Wt. (-24.68%) shows that a decrease in it will lead to increase in activity. The descriptor SsNH2E-index (22.59%) is directly proportional to the activity; this descriptor signifies electro topological state indices for number of $–NH_2$ group connected with one single bond. Finally descriptor T_O_F_5 (13.45%) is an influential descriptor and is directly proportional to the activity which signifies the count of number of oxygen atom separated from fluorine atom by 5 bonds in a molecule.

The plot of observed versus predicted activity (Figure 5) showed that the model is able to predict the activity of training set quite well (all points close to the regression line) as well as external test set (all points close to the regression line) providing confidence in predictive ability of the model.

Unicolumn Statistics is a method to analyze the descriptor data to check data spread by calculating mean and standard deviation for both training dataset as well as test set. The result of Unicolumn statistics for model is given in Table No. 3.

The min and max values in both training and test should be compared in a way that:

•The max of the test should be less than max of training set.
•The min of the test should be greater than min of training set.

Unicolumn statistics of model shows that the test set is interpolative i.e. derived within the min-max range of the training set. The mean and standard deviation of the training and test set provides insight to the relative difference of mean and point density distribution (along mean) of the two sets. Also, a relatively higher standard deviation in training set indicated that training set has widely distributed activity of the molecules as compared to the test set. Correlation matrix showed the measure of dependence between the two descriptors (Table No.4). The actual and predicted activity with residual of model is shown in Table 5.

3.2 3D–QSAR studies

3-D QSAR analysis was performed using kNN – MFA with stepwise forward- backward variable selection method. The model summary is given in Table 6.

The model explains internal (q^2 = 0.5493) as well as external (prd r^2 = 0.3418) model validation and prediction. The model consisted of two electrostatic descriptor and one steric descriptor with kNN (k=2). The electrostatic and steric descriptors at the grid showed the relative position and ranges in the model providing guidelines for new molecule design (Figure- 6,7). Positive range in the electrostatic descriptor means that a positive electrostatic potential is favorable for biological activity. Negative range in the steric descriptors means that a less bulky substitution is favorable for biological activity. The actual and predicted activities with residual values are shown in Table 7.

Table 1. Imidazole analogues with HO-1 inhibitory activity

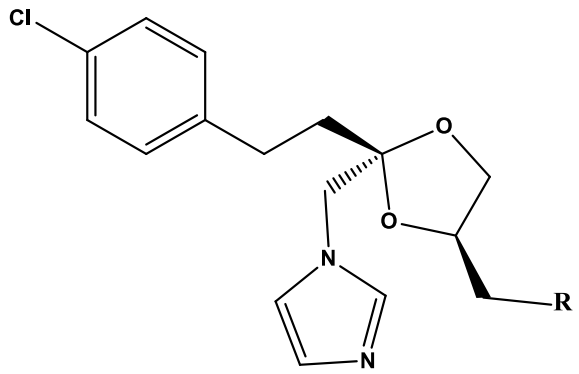

figure-1 Chemical structure of imidazole dioxolane

S.No.	R	IC_{50} (µM) of HO-1	pIC_{50} of HO-1
01.	Phenyl sulphanyl	1.03	-0.01283
02.	4-aminophenyl sulphanyl	0.33	0.48148
03.	2-aminophenyl sulphanyl	4	-0.60205
04.	3-aminophenyl sulphanyl	4	-0.60205
05.	Pyridin-4-yl sulphanyl	25	-1.39794
06.	4-hydroxyphenyl sulphanyl	1.59	-0.20139
07.	4-bromophenyl sulphanyl	2.1	-0.32221
08.	4-methoxyphenyl sulphanyl	0.7	0.15490
09.	4-chlorophenyl sulphanyl	2.8	-0.44715
10.	4-fluorophenyl sulphanyl	2.2	-0.34242
11.	4-nitrophenyl sulphanyl	6	-0.77815
12.	(5-trifluoromethyl)pyridin-2 yl sulphanyl	2.1	-0.32221
13.	cyclohexyl sulphanyl	0.94	0.02687
14.	naphthalene-2-yl sulphanyl	0.9	0.04575
15.	3-bromophenyl sulphanyl	5	-0.69897
16.	2-bromophenyl sulphanyl	6	-0.77815
17.	4-aminophenoxy	1.4	-0.14612
18.	4-hydroxyphenoxy	1.8	-0.25527
19.	Phenoxy	0.59	0.22914
20.	4-bromophenoxy	3.5	-0.54406
21.	4-fluorophenoxy	0.28	0.55284
22.	Biphenyl-4-yl oxy	2	-0.30102
23.	4-methoxyphenoxy	1.33	-0.12385
24.	4-iodophenoxy	9	-0.95424
25.	4-cyanophenoxy	0.67	0.17392

Table 2. Grid Settings.

Grid Setting	From	To	Interval
X	-4.881500	20.057900	2.0000
Y	-7.056700	16.736500	2.0000
Z	-7.959000	8.692700	2.0000

Table 3. Unicolumn Statistics

	Column name	**Average**	**Max**	**Min**	**Std Dev.**	**Sum**
Training	pIC_{50}	-0.2811	0.5528	-1.3979	0.4962	-5.0592
Test	pIC_{50}	-0.4011	0.1739	-0.7782	0.3725	-2.0056

Table 4. Correlation matrix of Descriptors

	Mol. Wt.	**SsNH2E-index**	**T_N_O_7**	**T_O_F_5**
Mol. Wt.	1			
SsNH2E-index	-0.18064	1		
T_N_O_7	-0.25501	0.443648	1	
T_O_F_5	-0.21914	-0.08574	-0.08575	1

Table 5. Actual and predicted activity [pIC_{50}] with residual of model

Molecule	**Actual (pIC_{50})**	**Prediction**	**Residual**
DG01	-0.01283	-0.01565	0.00282
DG02	0.48148	0.588312	-0.106832
DG03*	-0.60205	-0.62844	0.02639
DG04	-0.60205	-0.65409	0.05204
DG05	-1.39794	-1.28131	-0.11663
DG06	-0.20139	-0.13487	-0.06652
DG07	-0.32221	-0.60358	0.28137
DG08	0.1549	-0.2394	0.39430
DG09	-0.44715	-0.27233	-0.17482
DG10	-0.34242	-0.14971	-0.19271
DG11	-0.77815	-0.35097	-0.42718
DG12	-0.32221	-0.52973	0.20752
DG13	0.02687	-0.06071	0.08758
DG15	-0.69897	-0.60358	-0.09539

DG16*	-0.77815	-0.60358	-0.17457
DG18*	-0.25527	-0.01515	-0.24012
DG19	0.22914	0.104081	0.125059
DG20*	-0.54406	-0.48385	-0.06021
DG21	0.55284	0.561171	-0.00833
DG22	-0.30102	-0.463	0.16198
DG23	-0.12385	-0.11967	-0.00418
DG24	-0.95424	-0.83412	-0.12012
DG25*	0.17392	-0.08229	0.25621

* indicates compounds of test set

Table 6. Statistics value of 3-D model

kNN = 2	n = 16	Degree of freedom = 12
q^2 = 0.5493	q^2 se =0.3557	
Prd r^2 = 0.3358	Prd r^2se = 0.3418	
Descriptor Range: E_834 (2.9876, 3.2702) E_932 (9.2356, 9.9801) S_601 (-0.5045, -0.5044)		

Table 7: Actual and predicted activities [pIC_{50}] with residual values for the 3D- model

Molecule	**Actual (pIC_{50})**	**Prediction**	**Residual**
DG01	0.01283	-0.23676	0.22393
DG02*	0.48148	-0.10683	0.58831
DG03*	-0.60205	-0.74143	0.139384
DG04 *	-0.60205	-0.7328	0.130754
DG05	-1.39794	-0.67523	-0.722712
DG06	-0.20139	-0.08955	-0.111837
DG07	-0.32221	-0.39752	0.075311
DG08*	0.1549	-0.10674	0.261642
DG09	-0.44715	-0.33222	-0.114935
DG10	-0.34242	-0.38733	0.044905
DG11	-0.77815	-1.13374	0.35559
DG12*	-0.32221	-0.38462	0.062407
DG13	0.02687	0.189304	-0.162434
DG15	-0.69897	-0.77813	0.079162
DG16	-0.77815	-0.68554	-0.092608
DG18*	-0.25527	-0.75054	0.495265
DG19	0.22914	-0.10923	0.338373
DG20	-0.54406	-0.91203	0.367971
DG21	0.55284	0.080772	0.472068
DG22*	-0.30102	-0.32609	0.025066
DG23	-0.12385	0.360731	-0.484581
DG24	-0.95424	-0.52521	-0.429033
DG25	0.17392	0.337069	-0.163149

* indicates compounds of test set

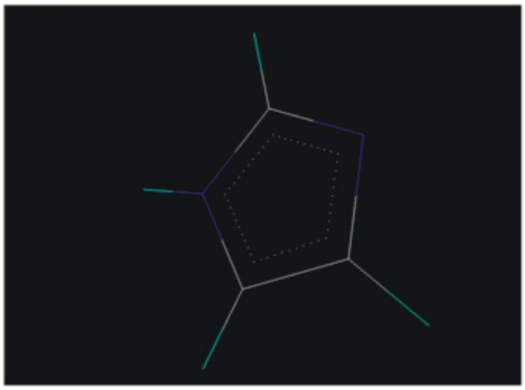

Figure 2: Imidazole template

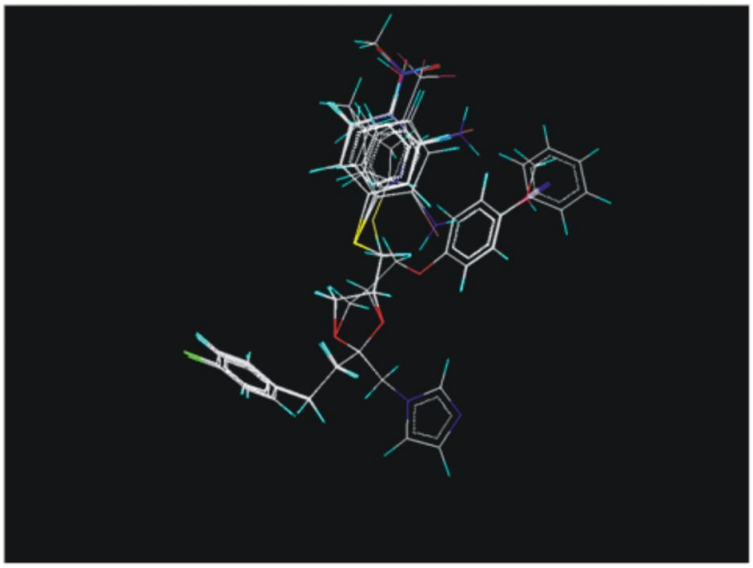

Figure: 3 Alignment of molecules of series

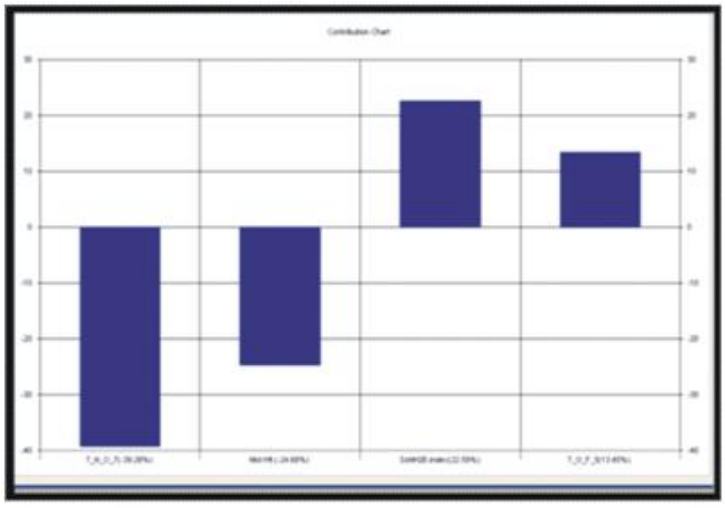

Figure 4 Contribution Chart of model

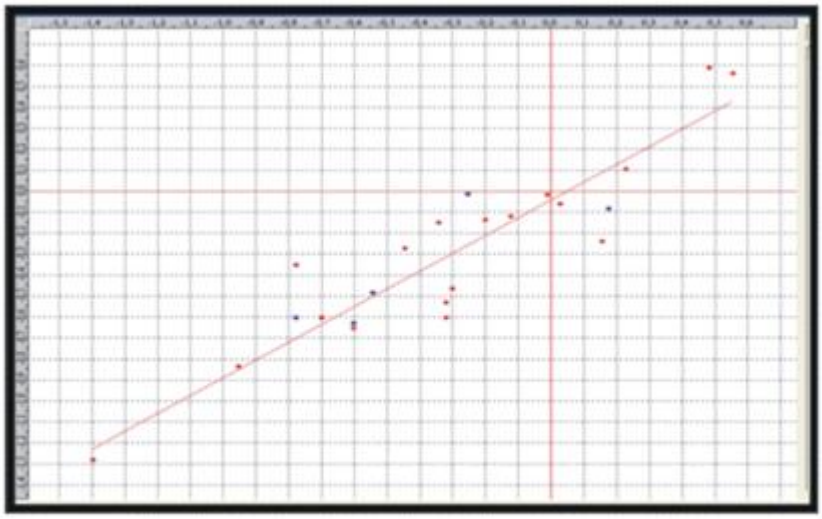

Figure 5: Fitness plot *between actual and Predicted Activities for model training set (red spots) and test set (blue spots)*

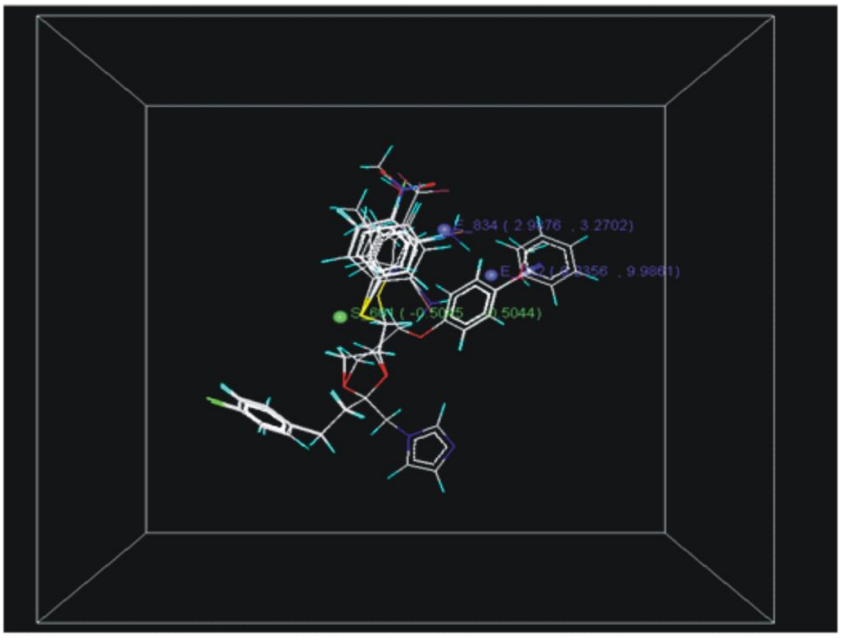

GRID OF 3D- QSAR MODEL:

Figure 6: Distribution of point in the SW kNN-MFA

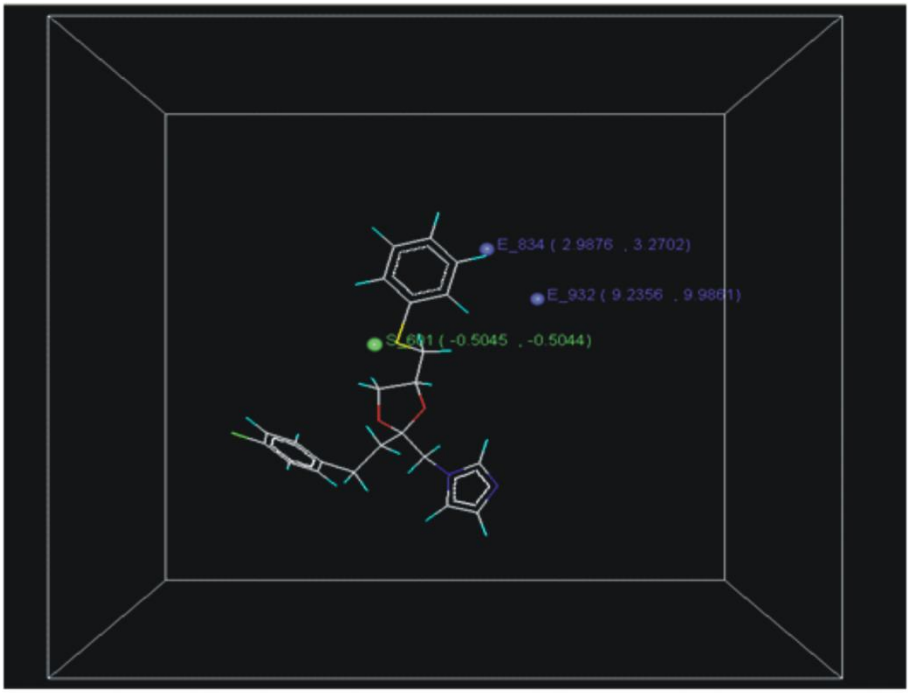

Figure 7: Distribution of point in the lead molecule

4. CONCLUSION

An imidazole-dioxolane compound has emerged as a potential therapeutic agent for Heme Oxygenase inhibition. So the present work focused on the QSAR analysis on some novel imidazole derivatives for the development of potent Heme Oxygenase inhibitor with the help of software. The 2-D QSAR analysis suggested four descriptors, Molecular weight, SsNH2E index, T_N_O_7 and T_O_F_5 contributed to the biological activity. Out of the four descriptors Molecular weight and T_N_O_7 contributed negatively while SsNH2E index and T_O_F_5 contributed positively. The model showed good statistical values and correlation matrix of the descriptors. The 3-D descriptors electrostatic and steric revealed the relative positions and range for substitution in a molecule. In 3D model, grid suggested that a positive electrostatic potential is favorable for increase in biological activity and the steric field with negative range and the negative range indicates that negative steric potential is favorable for increase in the activity. So, with the help of 2D and 3D data, some new molecules can be designed in order to get a potent compound.

ACKNOWLEDGEMENT

Darshana Gohate, one of the authors, is thankful to Department of Pharmacy, Barkatullah University for providing the necessary facilities to carry out this research work.

REFERENCES

1. Alam J, Igarashi K, Immenschuh S, Shibahara S,Tyrrell RM. Regulation of heme oxygenase-1 gene transcription: Recent advances and highlights from the International conference. Antioxid. & Red. Signal. 2004; 6: 924-933.
2. Roman G, Riley JG, Vlahakis JZ, Kinobe RT, Brien JF, Nakatsu K, Szarek WA. Heme oxygenase inhibition by 2-oxy-substituted 1-(1H-imidazol-1-yl)-4-phenylbutanes: Effect of halogen substitution in the phenyl ring. Bioorg. & Med. Chem. 2007; 15: 3225–3234.
3. Vlahakis JZ, Kinobe RT, Bowers RJ, Brien JF, Nakatsu K, Szarek WA. Synthesis and evaluation of azalanstat analogues as heme oxygenase inhibitors. Bioorg. & Med. Chem. Lett. 2005; 15:1457–1461.
4. Cashore WJ, Oh W. Unbound Bilirubin and Kernicterus in Low-Birth-Weight Infants. Pediatrics. 1982; 69: 481–485.

5. Bhutani VK, Performance evaluation for neonatal phototherapy. Ind. Pediatrics. 2009; 46: 19-21.
6. Cohen AN, Ostrow JD.New Concepts in Phototherapy: Photoisomerization of Bilirubin IXα and Potential Toxic Effects of Light, Pediatrics. 1980; 65:740–750.
7. Rosenstein BS, Ducore JM. Enhancement by bilirubin of DNA damage induced in human cells exposed to phototherapy light. Pediatric. Res. 1984; 18: 3–6.
8. Moseley MJ, Fielder AR.Phototherapy: an ocular hazard revisited. Arch. Dis. Child. 1988; 63: 886–887.
9. Chen M, Regan RF. Time course of increased heme oxygenase activity and expression after experimental intracerebral hemorrhage: correlation with oxidative injury. J. Neurochem. 2007; 103: 2015–2021.
10. Gong Y, Tian H, Xi G, Keep RF, Hoff JT, Hua Y. Systemic zinc protoporphyrin administration reduces intracerebral hemorrhage-induced brain injury. Acta. Neurochir. Suppl. 2006; 96: 232–236.
11. Wagner KR, Hua Y, Courten-Myers GM , Broderick JP, Nishimura RN, Lu SY, Dwyer BE. Tin-mesoporphyrin, a potent heme oxygenase inhibitor, for treatment of intracerebral hemorrhage: in vivo and in vitro studies. Cell Mol. Biol. 2000;46: 597–608.
12. Fang J, Sawa T,AkaikeT . *In vivo antitumor activity of pegylated zinc protoporphyrin: targeted inhibition of heme oxygenase in solid tumor*. Cancer Res. 2003; 63: 3567-74.
13. Tanaka S, Akaike T, Fang J, Beppu T, Ogawa M, Tamura F, Miyamoto Y, Maeda H, Antiapoptotic effect of haem oxygenase-1 induced by nitric oxide in experimental solid tumour. Br. J. Cancer. 2003; 88: 902-09.
14. Fang J , Akaike T, Maeda H. Antiapoptotic role of heme oxygenase (HO) and the potential of HO as a target in anticancer treatment. Apoptosis. 2004: 9: 27-35.
15. Vlahakis JZ, Kinobe RT, Bowers RJ, Brien JF, Nakatsu K, Szarek WA. Imidazole-Dioxolane Compounds as Isozyme-Selective Heme Oxygenase Inhibitors. J. Med. Chem. 2006; 49: 4437-4441.
16. Maines MD. The heme oxygenase system: A regulator of second messenger gases, Ann. Rev.of Pharmacol. & Toxicol. 1997;37: 517-554.
17. Kinobe RT, Vlahakis JZ, Vreman HJ, Stevenson DK, Brien JF, Szarek WA, Nakatsu K. Selectivity of imidazole–dioxolane compounds for in vitro inhibition of microsomal haem oxygenase isoforms. Brit. J. of Pharmacol. 2006; 147: 307–315.
18. DeNagel DC, Verity AN, Madden FE, Yang CO, Sangameswaran L, Johnson RM. Identification of non-porphyrin inhibitors of heme oxygenase-1. Society for Neurosci. 1998; 24: 2058.
19. Tuck SF, Patel H, Safi E, Robinson CH. Lanosterol 14 alpha-demethylase (P45014DM): effects of P45014DM inhibitors on sterol biosynthesis downstream of lanosterol. J. of Lip. Res. 1991; 32: 893.
20. Jain KS, Kathiravan MK, Somania RS, Shishoo CJ. The biology and chemistry of hyperlipidemia. Bioorg. & Med. Chem. 2007; 15:4674–4699.
21. Zhang F, Kaide JI, Rodriguez-Mulero F, Abraham NG, Nasjletti A. Vasoregulatory function of the heme-heme oxygenase-carbon monoxide system. Am. J. of Hyperten. 2001; 14: 62S-67S.
22. Mghazli S, Jaouad A, Mansour M, Villemin D, Cherqaoui D. Neural Networks Studies:quantitative structure-activity relationships of antifungal 1-[2-(substituted phenyl)allyl]imidazoles and related compounds. Chemosph. 2001; 43: 385-390.
23. Miranda PO, Gundersen LL. Synthesis of Imidazole Derivatives with Antimycobacterial Activity.Arch. Pharm. Chem. Life Sci. 2010; 343: 40-47.
24. Lean TH, Vengadasalam D. Treatment of vaginal trichomoniasis with a new anti-protozoal compound (-chloromethyl-2-methyl-5-nitro-1-imidazole-ethanol). Brit. J. of Veneral Diseases. 1973; 49: 69-71.
25. Palin R, Clark JK, Evans L, Houghton AK, Jones PS, Prosser A, Wishart G, Yoshiizumi K. Structure–activity relationships and CoMFA of N-3 substituted phenoxypropyl piperidine benzimidazol-2-one analogues as NOP receptor agonists with analgesic properties. Bioorg. & Med. Chem. 2008; 16: 2829–2851.
26. Wachall BG, Hector M, Zhuang Y, Hartmann RW. Imidazole substituted biphenyls: A new class of highly potent and in vivo active inhibitors of P450 17 as potential therapeutics for treatment of prostate cancer. Biorg. and Med. Chem. 1999; 7: 1913-1924.
27. Yoo SE, Kim SK, Lee SH, Yi KY, Lee DW, A comparative molecular field analysis and molecular modelling studies on pyridylimidazole type of angiotensin II antagonists. Bioorg. & Med. Chem. 1999;7: 2971-2976.

28. Hadizadeh F, Hosseinzadeh H, Shariaty VSM, Seifi M, Kazemi S. Synthesis and Antidepressant Activity of N-Substituted Imidazole-5-Carboxamides in Forced Swimming Test Model. Iranian J. of Pharm. Res. 2008; 7: 29-33.
29. Mor M, Bordi F, Silva C, Rivara S, Zuliani V, Vacondio F, Rivara M, Barocelli E, Bertoni S, Ballabeni V, Magnanini F, Impiciatore M, Plazzi PV. Synthesis, biological activity, QSAR and QSPR study of 2-aminobenzimidazole derivatives as potent H_3-antagonists. Biorg. and Med. Chem. 2004; 12: 663-674.
30. Clough DP, Hatton R, Pettinger SJ, Samuels GM, Shaw A. Substituted aryl-tetrahydro-pyrrolo imidazoles: a new class of centrally acting antihypertensives. Brit. J. Pharmacol. 1978; 62: 385P-386P.
31. Sugishima M, Higashimoto Y, Oishi T, Takahashi H, Sakamoto H, Noguchi M, Fukuyama K. X-ray Crystallographic and Biochemical Characterization of the Inhibitory Action of an Imidazole−Dioxolane Compound on Heme Oxygenase. Biochemistry. 2007; 46: 1860–1867.
32. Rahman MN, Vlahakis JZ, Szarek WA, Nakatsu K, Jia Z. X-ray crystal structure of human heme oxygenase-1 in complex with 1-(adamantan-1-yl)-2-(1H-imidazol-1-yl)ethanone: a common binding mode for imidazole-based heme oxygenase-1 inhibitors. J. Med. Chem. 2008; 51: 5943–5952.
33. Rahman MN, Vlahakis JZ, Vukomanovic D, Szarek WA, Nakatsu K, Jia Z. X-ray crystal structure of human heme oxygenase-1 with (2R, 4S)-2-[2-(4-chlorophenyl)ethyl]-2-[(1H-imidazol-1-yl)methyl]-4[((5-trifluoromethylpyridin-2-yl)thio)methyl]-1,3-dioxolane: a novel inducible binding mode. *J. Med. Chem.* 2009; 52: 4946–4950.
34. Roman G, Rahman MN, Vukomanovic D, Jia Z, Nakatsu K, Szarek W. Heme oxygenase inhibition by 2-oxy-substituted 1-azolyl-4-phenylbutanes: effect of variation of the azole moiety. X-ray crystal structure of human heme oxygenase-1 in complex with 4-phenyl-1-(1H-1,2,4-triazol-1-yl)-2-butanone. Chem. Biol. Drug Des. 2010; 75: 68-90.
35. Rahman MN, Vlahakis JZ, Roman G, Vukomanovic D, Szarek WA, Nakatsu K, Jia Z. Structural characterization of human heme oxygenase-1 in complex with azole-based inhibitors. J. of Inorg. Biochem. 2010; 104: 324-330.
36. Vlahakis JZ, Humb M, Rahman MN , Jia Z, Nakatsu K , Szarek WA. Synthesis and evaluation of imidazole–dioxolane compounds as selective heme oxygenase inhibitors: effect of substituents at the 4-position of the dioxolane ring. Bioorg. & Med. Chem. 2009; 17: 2461–2475.
37. VLife MDS 3.5, Molecular Design Suite, VLife Sciences Technologies Pvt. Ltd., Pune, India, (www.vlifesciences.com)
38. Ajmani S, Jadhav K, Kulkarni SA. Three-Dimensional QSAR Using the k-Nearest Neighbor Method and Its Interpretation. J. Chem. Inf. Model. 2006; 46: 24-31.